

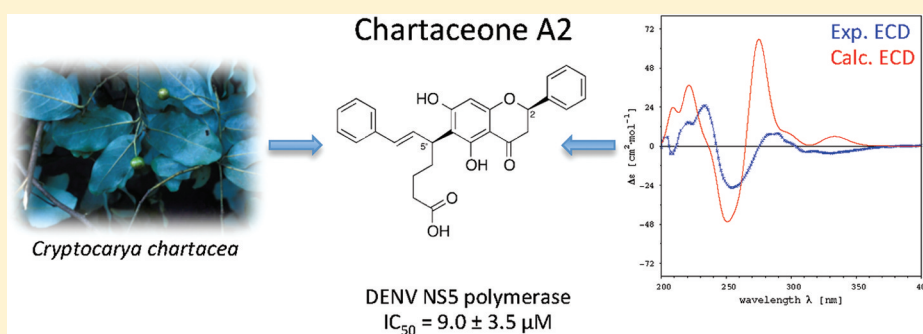
Alkylated Flavanones from the Bark of *Cryptocarya chartacea* As Dengue Virus NS5 Polymerase Inhibitors

Pierre-Marie Allard,[†] Elise Tran Huu Dau,[†] Cécilia Eydoux,[‡] Jean-Claude Guillemot,[‡] Vincent Dumontet,[†] Cyril Poullain,[†] Bruno Canard,[‡] Françoise Guéritte,[†] and Marc Litaudon^{*,†}

[†]Centre de Recherche de Gif, Institut de Chimie des Substances Naturelles, CNRS, 1 Avenue de la Terrasse, 91198 Gif-sur-Yvette Cedex, France

[‡]AFMB, Aix-Marseille University, CNRS, UMR 6098, ESIL 13228, Marseille, France

Supporting Information



ABSTRACT: An in vitro screening of New Caledonian plants allowed the selection of several species with a significant dengue virus NS5 RNA-dependent RNA polymerase (RdRp) inhibiting activity. The chemical investigation of *Cryptocarya chartacea* led to the isolation of a series of new mono- and dialkylated flavanones named chartaceones A–F (1–6), along with pinocembrin. They were isolated as racemic mixtures and characterized using extensive one- and two-dimensional NMR spectroscopy. Four diastereomers of chartaceone A (1) were separated using chiral HPLC, and their absolute configurations were established by comparison of their experimental and calculated ECD spectra. The dialkylated flavanones, chartaceones C–F (3–6), exhibited the most significant NS5 RdRp inhibiting activity, with IC_{50} ranging from 1.8 to 4.2 μM . Chartaceones represent a new class of non-nucleosidic inhibitors of the DENV NS5 RdRp.

The dengue virus (DENV) is responsible for dengue fever (DF) and dengue hemorrhagic fever (DHF), which are increasingly important public health problems in tropical and subtropical regions.¹ Worldwide, an estimated 2.5 billion people are at risk of infection and about 500 million infections occur each year, including 500 000 hospitalizations for DHF and 20 000 deaths.² Despite the importance of this disease, no vaccine or specific antiviral is available.³ The development of an effective therapeutic agent against DENV is crucial. The RNA-dependent RNA polymerase (RdRp) domain of the non-structural protein 5 (NS5) of the DENV appears as a promising target for new drugs since polymerase activity is essential for viral replication and human host cells are devoid of such RdRp activity.⁴ To date, *N*-sulfonylanthranilic acid derivatives are the only non-nucleosidic DENV NS5 polymerase inhibitors that have been reported.⁵ Thus, there is an urgent need for the discovery of new efficient antiviral agents targeting the DENV to treat this disease.

In this context, a biological screening was conducted on 1350 EtOAc extracts prepared from various parts of approximately 650 New Caledonian plants using an assay⁶ adapted to high-throughput format. Among the active extracts, the bark of

Cryptocarya chartacea Kosterm., an endemic species of the family Lauraceae, was selected for chemical investigation due to its high potency.

Various secondary metabolites such as alkaloids,^{7,8} α -pyrones,^{9,10} and simple¹¹ and complex^{12–14} flavonoids have been isolated from several *Cryptocarya* species. Some of them have shown interesting biological properties such as antiviral,^{15,16} cytotoxic,¹⁷ or apoptosis inducer activities.¹⁸

In this paper, we report the isolation, characterization, and biological activities of pinocembrin and chartaceones A–F (1–6), a series of new 6-mono- and 6,8-dialkylated flavanones. The absolute configuration of four diastereomers of chartaceone A (1a–d) is also detailed.

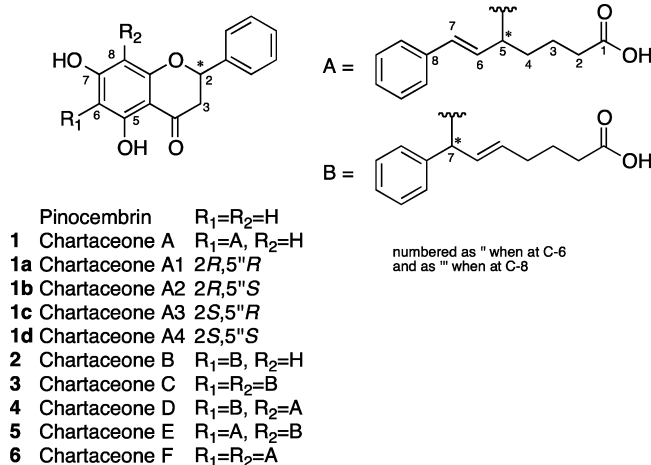
RESULTS AND DISCUSSION

Approximately 1350 EtOAc extracts previously filtered on polyamide cartridges were screened at 50 $\mu g/mL$ on a dengue polymerase assay using the RdRp domain of the DENV-2 NS5 protein.⁶ A second screen at 10 $\mu g/mL$ was carried out on 320

Received: September 1, 2011

Published: November 3, 2011

selected active extracts, of which 49 exhibited an enzyme inhibition of $\geq 80\%$. Interestingly, among these active extracts, several species of the genus *Cryptocarya* were found to possess a strong interaction with RNA polymerase, the EtOAc bark extract of *C. chartacea* showing significant antiviral activity (90% at 10 $\mu\text{g/mL}$). This extract was subjected to C_{18} flash chromatography eluted with a H_2O –MeOH gradient to afford 12 fractions. Subsequent semipreparative and preparative HPLC on the active fractions afforded the known pinocembrin and chartaceones A–F (1–6). All the compounds were isolated as optically inactive mixtures.



Chartaceones A (1) and B (2) were obtained as yellow, amorphous solids. The same molecular formula, $C_{28}H_{26}O_6$, for chartaceones A (1) and B (2) was deduced from their HR-ESIMS quasi-molecular ion peak $[M - H]^-$ at m/z 457.1671 and 457.1653, respectively (calcd 457.1651). The UV spectra of chartaceones A (1) and B (2) showed absorption bands at 290 and 340 nm (shoulder) consistent with a flavanone core,¹⁹ but with an additional absorption band at 250 nm, indicating the presence of a styrene moiety²⁰ in the case of chartaceone A (1). The flavanone moiety was confirmed in the 1H NMR spectra (see Table 1) by the presence of a typical ABX system for H-2 and H-3 (δ_H 5.43, dd, $J = 12.9$ and 3.1 Hz, δ_H 2.75, dd, $J = 17.1$ and 3.1 Hz, and δ_H 3.08, dd, $J = 17.1$ and 12.9 Hz) for chartaceone A (1) and (δ_H 5.44, dd, $J = 12.9$ and 3.1 Hz, δ_H 2.75, dd, $J = 17.1$ and 3.1 Hz, and δ_H 3.09, dd, $J = 17.1$ and 12.9 Hz) for chartaceone B (2). Other NMR data (see Tables 1 and 2) are consistent with the presence of a pinocembrin carbon skeleton substituted by an arylheptanoid side chain at C-6, but with slight differences between chartaceones A and B (1 and 2). Indeed, HSQC, HMBC, and COSY correlations (Figure 1)

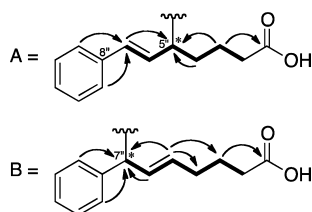


Figure 1. Key COSY (bold) and HMBC (arrows) correlations for side chains A and B (in compounds 1 and 2, respectively).

indicated that the side chain is an (*E*)-7-phenylhept-6-enoic acid moiety coupled at C-5 (type A) and an (*E*)-7-phenylhept-5-enoic acid moiety coupled at C-7 (type B) for chartaceones

A (1) and B (2), respectively. The substitution of the pinocembrin core at C-6 was confirmed by the following evidence: cross-peaks from C-5, C-6, and C-10 to the hydrogen-bonded OH-5 at ca. δ_H 12.50 and from C-5, C-6, and C-7 to the methine H-5'' (δ_H 4.05, q, $J = 8.0$ Hz) for chartaceone A (1) or H-7'' (δ_H 5.33, d, $J = 8.5$ Hz) for chartaceone B (2) were observed in the HMBC spectra of 1 and 2 (run in $CDCl_3$). The geometry of the Δ^6 (1) and Δ^5 (2) double bonds was assigned as *E* on the basis of the large coupling constant between H-6'' and H-7'' ($J = 15.9$ Hz) and between H-5'' and H-6'' ($J = 15.2$ Hz), respectively. Chartaceones A (1) and B (2) were optically inactive and thus racemic.

The racemic mixture of chartaceone A (1) (85 mg) was subjected to chiral semipreparative HPLC (chromatogram in Supporting Information) to afford four diastereomers obtained in a 1:1:1:1 ratio (ca. 20 mg each), chartaceones A1–A4 (1a–d), named by order of elution. Their absolute configurations were assigned by comparison of experimental and calculated ECD spectra. Two pairs of mirror-imaged ECD curves revealed the enantiomeric nature of chartaceones A1 and A4 (1a and 1d) and A2 and A3 (1b and 1c) (Figure 2).

The CD spectra of compounds 1a–d showed four Cotton effects (CE) (Figure 2). Transitions due to the aryl ketone chromophore²¹ of 2*S*-flavanones generate a positive CE in the $n \rightarrow \pi^*$ region (320–330 nm) and a negative CE in the $\pi \rightarrow \pi^*$ region (280–290 nm) of their ECD spectra, as shown by Gaffield.²² From the ECD spectra of chartaceones A1 (1a) and A2 (1b), which showed a negative CE at ca. 330 nm and a positive CE at ca. 290 nm, it could be deduced that both possess an *R* configuration at C-2, and chartaceones A3 (1c) and A4 (1d) conversely possess an *S* configuration at C-2. The comparison of the ECD spectra of chartaceones A1–A4 (1a–d) with that of 2*S*-pinocembrin²³ suggested that the observed CE at lower wavelengths (ca. 250 and 230 nm) originated from the chirality at C-5'' of the arylheptanoid side chain.

Time-dependent density functional theory at the B3LYP/6-31G** level has been shown to be a powerful method for calculating the ECD spectra of flavonoids.^{24,25} Therefore, theoretical calculations were engaged to determine the contribution of chirality at C-5'' for chartaceones A1–A4 (1a–d).

A conformational study was undertaken on (2*R*,5''*R*)- and (2*R*,5''*S*)-configured chartaceones A. After selection of the lowest energy conformers, overall ECD curves for both configurations were simulated. Calculated molecular orbitals of these structures confirmed that the diagnostic CEs at 250 nm and 220–230 nm originated by electronic perturbation of the styrene chromophore at C-5''. Quantum chemically predicted ECD and experimental spectra of 2*R*,5''*R*-chartaceone A1 (1a) and 2*R*,5''*S*-chartaceone A2 (1b) are shown Figure 3. In the 350–280 nm region, mainly influenced by the C-2 chirality, the adequacy of calculated and experimental ECD curves for chartaceones A1 (1a) and A2 (1b) is approximate. On the other hand, in the lower wavelength part of the spectrum, supposedly influenced by the styrene chromophore at C-5'', a positive CE at ca. 255 nm and negative CE at ca. 220 nm were observed for the calculated ECD curve of the 2*R*,5''*R*-configured compound and experimental ECD curve of compound 1a, indicating that the absolute configuration of chartaceone A1 (1a) could be assigned as 2*R*,5''*R*. Likewise, similar experimental and calculated ECD curves for compound 1b (2*R*,5''*S*-configured compound) allowed the absolute configuration of chartaceone A2 (1b) to be assigned as 2*R*,5''*S*. From these results and taking into account that compounds 1a and

Table 1. ¹H NMR Data (methanol-*d*₄, 300 MHz) for Chartaceones A (1a–d)^a and B–F (2–6)^b

position	1a–d	2	3	4	5	6
	δ_{H} (J in Hz)	δ_{H} (J in Hz)	δ_{H} (J in Hz)	δ_{H} (J in Hz)	δ_{H} (J in Hz)	δ_{H} (J in Hz)
2 ^c	5.43, dd (12.9, 3.1)	5.44, dd (12.9, 3.1)	5.09, d (13.0) 5.39, d (12.7)	5.51, d (12.9) 5.41, d (12.9)	5.12, m 5.42, d (13.0)	5.44, d (12.9) 5.33, d (12.9)
3 α	2.75, dd (17.1, 3.1)	2.75, dd (17.1, 3.1)	2.71, d (16.6)	2.78, d (16.9)	2.75, d (16.6)	2.75, d (16.9)
3 β^c	3.08, dd (17.1, 12.9)	3.09, dd (17.1, 12.9)	2.86, dd (16.6, 13.0) 3.05, dd (16.6, 12.7)	3.09, dd (16.9, 12.9) 3.16, dd (16.9, 12.9)	2.90, m 3.08, dd (16.6, 13.0)	3.03, dd (16.9, 12.9) 3.11, dd (16.9, 12.9)
8	6.00, s	6.00, s				
2'	7.48, d (8.0)	7.49, d (8.0)	7.10–7.29, m	7.53, d (7.0)	7.07–7.33, m	7.49, d (7.1)
3'	7.35–7.43	7.32–7.44	7.10–7.29, m	7.36–7.46, m	7.07–7.33, m	7.41, t (7.1)
4'	7.35–7.43	7.32–7.44	7.10–7.29, m	7.36–7.46, m	7.07–7.33, m	7.37, m
5'	7.35–7.43	7.32–7.44	7.10–7.29, m	7.36–7.46, m	7.07–7.33, m	7.41, t (7.1)
6'	7.48, d (8.0)	7.49, d (8.0)	7.10–7.29, m	7.53, d (7.0)	7.07–7.33, m	7.49, d (7.1)
2''	2.30, m	2.31, t (7.2)	2.15–2.36, m	2.30, m	2.37, m	2.20–2.34, m
3''	1.57, m	1.71, qt (7.2)	1.57–1.76, m	1.71, m	1.56–1.65, m	1.50–1.67, m
4''	1.87, m	2.14, q (7.2)	2.00–2.22, m	2.17, m	1.95–2.04, m	1.91–2.08, m
5''	2.03, m					
5''	4.05, q (8.5)	5.56, ddd (15.2, 8.7, 7.2)	5.45–5.65, m	5.60, m	4.05, m	4.06, m
6'' ^c	6.74, dd (15.9, 8.5) ^d 6.72, dd (15.9, 8.5) ^e	6.31, dd (15.2, 8.7) 6.30, dd (15.2, 8.7)	5.99–6.18, m	6.28, m	6.43, d (16)	6.73–6.80, m
7''	6.41, d (15.9)	5.16, d (8.7)	5.18, d (7.4)	5.26, m	6.8, m	6.44, d (15.7)
9''	7.32, d (7.4)	7.15–7.25	7.10–7.29, m	7.08–7.30, m	7.07–7.33, m	7.25–7.34, m
10''	7.24, t (7.4)	7.15–7.25	7.10–7.29, m	7.08–7.30, m	7.07–7.33, m	7.20–7.24, m
11''	7.13, t (7.4)	7.08, t (7.3)	7.10–7.29, m	7.08–7.30, m	7.07–7.33, m	7.08–7.16, m
12''	7.24, t (7.4)	7.15–7.25	7.10–7.29, m	7.08–7.30, m	7.07–7.33, m	7.20–7.24, m
13''	7.32, d (7.4)	7.15–7.25	7.10–7.29, m	7.08–7.30, m	7.07–7.33, m	7.25–7.34, m
2'''			2.15–2.36, m	2.25, m	2.22, m	2.20–2.34, m
3'''			1.57–1.76, m	1.55, m	1.67, m	1.50–1.67, m
4'''			2.00–2.22, m	1.85–1.98, m	2.06–2.12, m	1.70–1.90, m
5'''			5.45–5.65, m	3.98, m	5.56, m	4.01, m
6''' ^c			6.22–6.34, m	6.55–6.63, m	6.10, m	6.56, dd (15.9, 7.6) 6.65, dd (15.9, 7.6)
7''' ^c			5.26, d (7.5)	6.32, d (16.8) 6.35, d (16.8)	5.20, m	6.33, d (15.9) 6.36, d (15.9)
9'''			7.10–7.29, m	7.08–7.30, m	7.07–7.33, m	7.25–7.34, m
10'''			7.10–7.29, m	7.08–7.30, m	7.07–7.33, m	7.20–7.24, m
11'''			7.10–7.29, m	7.08–7.30, m	7.07–7.33, m	7.08–7.16, m
12'''			7.10–7.29, m	7.08–7.30, m	7.07–7.33, m	7.20–7.24, m
13'''			7.10–7.29, m	7.08–7.30, m	7.07–7.33, m	7.25–7.34, m

^aNMR data for optically pure chartaceones 1a–d. ^bNMR data for diastereomeric mixtures. ^cPossibility of the presence of two sets of signals of equal intensity for compounds 3–6. ^dChemical shifts for chartaceones 1a and 1d. ^eChemical shifts for chartaceones 1b and 1c.

1d, and 1b and 1c are enantiomers, the absolute configuration of chartaceones A3 (1c) and A4 (1d) could be assigned as 2*S*,5''*R* and 2*S*,5''*S*, respectively.

Chartaceone B (2) (44.9 mg) was similarly subjected to chiral semipreparative HPLC to afford the four diastereomeric chartaceones B1–B4 in a 1:1:1:1 ratio (ca. 10 mg each). Two pairs of mirror-imaged ECD curves (see Supporting Information) revealed the enantiomeric nature of chartaceones B1 and B4, and B2 and B3. As it is the case for chartaceones A1–A4, the absolute configuration at C-2 could be assigned as 2*R* (chartaceones B1 and B2) and 2*S* (chartaceones B3 and B4) from the CEs observed at 320 and 290 nm. On the other hand, the lack of clear CEs in the 250 nm region due to the absence of a styrene moiety did not allow assignment of the absolute configuration at C-7''.

Chartaceones C–F (3–6) were obtained as yellow to brownish, amorphous powders with the molecular formula C₄₁H₄₀O₈ being established by HR-ESIMS. It could be deduced from the molecular formula and spectroscopic data that

compounds 3–6, in addition to the arylheptanoid moieties at C-6, possess an additional arylheptanoid side chain at C-8. The comparison of the overall ¹H and ¹³C NMR data (Tables 1 and 2) of compounds 3–6 with those of 1 and 2 revealed substantial similarities, indicating that the additional side chain was either (*E*)-7-phenylhept-6-enoic acid or (*E*)-7-phenylhept-5-enoic acid. The lack of optical activity and the presence of three stereogenic centers suggested the racemic nature of chartaceones C–F (3–6). Several attempts of purification of the diastereomers using various chiral and nonchiral columns were unsuccessful. Thus, chartaceones C–F (3–6) are described as diastereomeric mixtures.

The absence of an absorption band at ca. 250 nm for a styrene moiety in the UV spectrum and the presence of two methine protons at δ_{H} 5.18 and 5.26 (H-7'' and H-7''', respectively) in the ¹H NMR spectrum of chartaceone C (3) indicated substitution by two 7-phenylhept-5-enoic acid moieties. The location of the side chains was supported by

Table 2. ^{13}C NMR Data (methanol- d_4 , 75 MHz) for Chartaceones A (1a–d)^a and B–F (2–6)^b

position	1a–d	2	3	4	5	6
	δ_{C}	δ_{C}	δ_{C}	δ_{C}	δ_{C}	δ_{C}
2 ^c	80.6	80.6	80.2	80.6 and 80.9	80.2	80.5 and 80.8
3 ^c	44.5	44.5	44.8	44.5 and 44.7	44.2 and 44.8	44.6 and 44.7
4 ^c	197.7	197.7	198.3 and 198.6	198.5 and 198.7	198.4 and 198.7	198.5 and 198.8
5 ^c	163.1	163	161.3	161.1 and 161.2	161.7	161.5 and 161.6
6 ^c	111.6	112.6	112.1 and 112.2	112.7	112.5	112.3
7 ^c	166.4	166.1	162.9 and 163	163.2	163.1 and 163.2	163.2 and 163.3
8 ^c	96.1	96.1	112.5 and 112.7	111.7	111.8	111.5 and 111.8
9 ^c	162.8	162.8	160.1 and 160.3	160.5 and 160.7	160.1	160.3 and 160.4
10 ^c	103.5	103.5	104.2 and 104.4	104.3	104.1 and 104.4	104.1 and 104.3
1 ^c	140.7	140.7	140.1 and 140.6	140.6 and 140.8	140.4	140.6 and 140.9
2'	127.5	127.5	126.8–129.6	127.7	126.8–129.7	127.6
3'	129.8	129.8	126.8–129.6	129.7–130	126.8–129.7	129.9
4'	129.7	129.7	126.8–129.6	129.7–130	126.8–129.7	129.8
5'	129.8	129.8	126.8–129.6	129.7–130	126.8–129.7	129.9
6'	127.5	127.5	126.8–129.6	127.7	126.8–129.7	127.6
1''	178.5	178.1	178.0	178.4	178.6	178.6
2''	35.5	34.6	34.7	34.9	35.6	35.6
3'' ^c	25	26.1	26.0 and 26.1	26.2	25	24.8 and 25
4'' ^c	33.7 ^e 33.8 ^d	33.1	33.0 and 33.1	33.1	33.7 and 33.8	33.7 and 33.8
5''	39.5	131.8	132.5 and 133.0	132.6 and 133	40	39.9
6'' ^c	134.1 ^d 134.2 ^e	133.1	132.5 and 133.0	132.6 and 133	130.8 and 130.9	133.8 and 133.9
7'' ^c	130.5	43.9	44.2 and 44.3	43.9	133.9	130.9
8'' ^c	139.7	145.6	145.0 and 145.1	144.6	139.5	139.4 and 139.5
9''	127.2	128.7	126.8–129.6	127.0–130.0	126.8–129.7	127.3
10''	129.6	128.8	126.8–129.6	127.0–130.0	126.8–129.7	129.6
11''	127.9	126.5	126.8–129.6	127.0–130.0	126.8–129.7	127.9–128.0
12''	129.6	128.8	126.8–129.6	127.0–130.0	126.8–129.7	129.6
13''	127.2	128.7	126.8–129.6	127.0–130.0	126.8–129.7	127.3
1'''			178.0	178.4	178.0	178.6
2'''			34.7	35.5	34.9 and 35	35.6
3''' ^c			26.0 and 26.1	24.8 and 24.9	26.1	24.8 and 25
4''' ^c			33.0 and 33.1	34.0 and 34.2	33 and 33.1	34.0 and 34.2
5''' ^c			132.5 and 133.0	39.7	132.5 and 132.9	39.7 and 39.8
6''' ^c			132.5 and 133.0	134.1 and 134.2	132.5 and 132.9	134.2 and 134.3
7'''			44.0	130.6	44.3	130.6
8''' ^c			144.6 and 144.7	139.4 and 139.5	145.2 and 145.3	139.4 and 139.5
9'''			126.8–129.6	127.0–130.0	126.8–129.7	127.3
10'''			126.8–129.6	127.0–130.0	126.8–129.7	129.6
11'''			126.8–129.6	127.0–130.0	126.8–129.7	127.9–128.0
12'''			126.8–129.6	127.0–130.0	126.8–129.7	129.6
13'''			126.8–129.6	127.0–130.0	126.8–129.7	127.3

^aNMR data for optically pure chartaceones 1a–d. ^bNMR data for diastereomeric mixtures. ^cPossibility of the presence of two sets of signals of equal intensity. ^dChemical shifts for chartaceones 1a and 1d. ^eChemical shifts for chartaceones 1b and 1c.

the HMBC correlations of H-7'' and H-7''' with C-6 and C-8, respectively.

An absorption band at ca. 250 nm in the UV spectrum of chartaceone F (6), together with the presence of two methine protons at δ_{H} 4.06 and 4.01 (H-5'' and H-5''', respectively) in its ^1H NMR spectrum, suggested substitution by two 7-phenylhept-6-enoic acid moieties. The location of the side chains was supported by the HMBC correlations of H-5'' and H-5''' with C-6 and C-8, respectively.

Planar structures of chartaceones D (4) and E (5) were obtained through the following evidence. In the ^1H NMR spectrum of chartaceones D (4) and E (5), typical signals at δ_{H} 3.98 and 5.26 (compound 4, H-5''' and H-7'', respectively) and

δ_{H} 4.05 and 5.20 (compound 5, H-5'' and H-7''', respectively) for methine protons of a 7-phenylhept-5-enoic acid and a 7-phenylhept-6-enoic acid moiety were observed. In the HMBC spectrum of 4 in DMF- d_7 , cross-peaks between H-7'' and the hydrogen-bonded OH at δ_{H} 13.14, and the quaternary C-5 (δ_{C} 161.0) and C-6 (δ_{C} 113.3), confirmed that the 7-phenylhept-5-enoic acid and the 7-phenylhept-6-enoic acid moiety were located at C-6 and C-8, respectively. In the HMBC spectrum of 5 in DMF- d_7 , cross-peaks between H-5'' and the hydrogen-bonded OH at δ_{H} 13.12, and the quaternary C-5 (δ_{C} 161.7) and C-6 (δ_{C} 112.7), confirmed that the 7-phenylhept-6-enoic acid moiety was located at C-6, and the 7-phenylhept-5-enoic acid moiety at C-8 (HMBC spectrum in the Supporting Information).

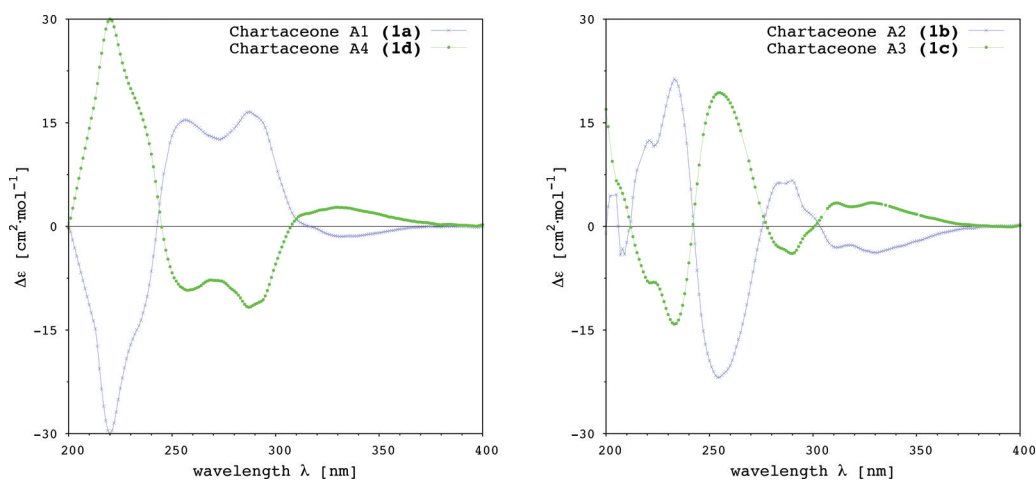


Figure 2. Experimental ECD curves of chartaceones A1–A4 (1a–d).

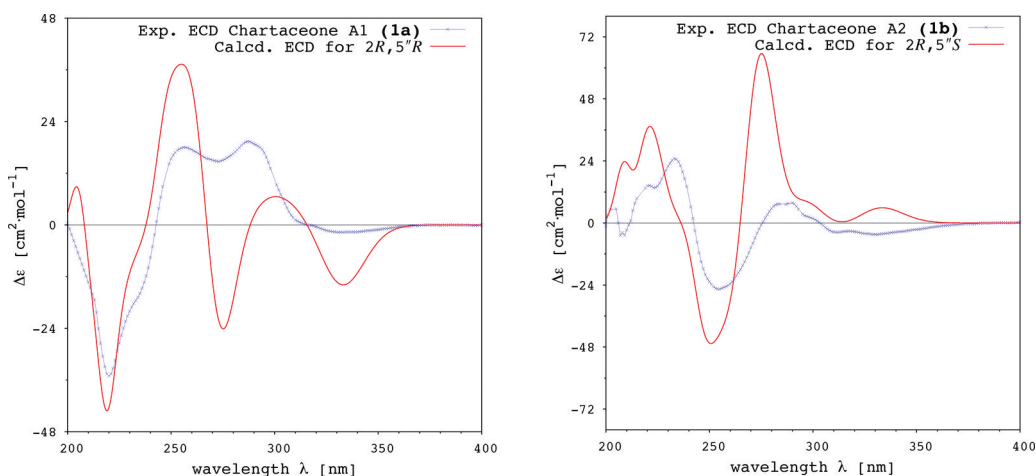


Figure 3. Left: Experimental and calculated ECD curves of chartaceone A1 (1a) and 2R,5'R-configured chartaceone A. Right: Experimental and calculated ECD curves of chartaceone A2 (1b) and 2R,5'S-configured chartaceone A.

In a similar way to calyxin A and B biosynthesis,²⁶ chartaceones A–F could be formed from the condensation of pinocembrin with an allylic intermediate originating from a phenylheptenoic acid.

Pinocembrin and all chartaceones A–F (1–6) were evaluated against DENV and bovine diarrhea virus (BVDV) NS5 polymerases (Table 3), both belonging to the family Flaviviridae. Polymerase activity was assayed by monitoring the incorporation of radiolabeled guanosine into a homopolymeric cytosine RNA template, as previously described.⁶ Their cytotoxicity was also evaluated against KB cell lines.

Some interesting observations emanated from these results. Pinocembrin and chartaceones A–F (1–6) are not cytotoxic in the KB cell line at 10 $\mu\text{g}/\text{mL}$. In the DENV polymerase assay, chartaceones C–F (3–6) showed significant IC_{50} 's ranging from 1.8 ± 1.2 to 4.2 ± 0.1 μM , whereas chartaceones A, A1–A4 (1, 1a–d) and B (2) were less active, and pinocembrin was not active, indicating that the presence of the arylheptanoid side chains at C-6 and C-8 plays an important role in the inhibition of the enzyme. In contrast, no inhibiting activity was shown for the BVDV polymerase, suggesting that the active compounds possess some selectivity toward DENV. Since the DENV polymerase inhibiting activities of compounds 3–6 were similar, it can be inferred that the two side chains play an equivalent role.

In conclusion, we have identified a novel series of mono- and dialkylated flavanones from the bark of *C. chartacea*, an

Table 3. Biological Activities of Pinocembrin and Chartaceones A–F (1–6)

compound	polymerase inhibition ^a		cytotoxicity ^b
	DENV	BVDV	KB
pinocembrin	not active		0
Chartaceone A (1)	14.8 ± 2.4	>50	3.2
Chartaceone A1 (1a)	15.3 ± 1.4	>50	0
Chartaceone A2 (1b)	9.0 ± 3.5	>50	11
Chartaceone A3 (1c)	27.0 ± 6.5	>50	0
Chartaceone A4 (1d)	7.4 ± 2.2	>50	6
Chartaceone B (2)	72.5 ± 15.3	>50	0
Chartaceone C (3)	4.2 ± 0.1	>50	0
Chartaceone D (4)	1.8 ± 1.2	>50	0
Chartaceone E (5)	2.9 ± 0.3	>50	0
Chartaceone F (6)	2.4 ± 0.3	>50	0
3'-deoxy-GTP ^c	0.02	<1	

^aDENV and BVDV NS5 polymerases: IC_{50} (μM) are mean values \pm SD ($n = 3$). ^bKB (nasopharynx human carcinoma cell line): % inhibition at 10 $\mu\text{g}/\text{mL}$. ^c3'-Deoxy GTP was used as a positive control of inhibition of both polymerases.

endemic species growing in New Caledonia. Chartaceones A–F exhibited moderate to potent enzyme-inhibiting activities on DENV NS5 polymerase and are not cytotoxic (KB cell line at 10 $\mu\text{g}/\text{mL}$). The presence of the arylheptanoid side chains at C-6 and C-8 is essential for a significant polymerase-inhibiting activity. Chartaceones represent a new class of non-nucleosidic inhibitors specific to the DENV NS5 RdRp.

EXPERIMENTAL SECTION

General Experimental Procedures. Optical rotations were measured at 25 °C on a JASCO P1010 polarimeter. The UV spectra were recorded on a Perkin-Elmer Lambda 5 spectrophotometer. ECD spectra were measured at 25 °C on a JASCO J-810 spectropolarimeter. The NMR spectra were recorded on a Bruker 300 MHz instrument (Avance 300) for compounds 1–6 and a Bruker 500 MHz instrument (Avance 500) for compounds 1a–d, using methanol- d_4 as solvent. Additional experiments were recorded on a Bruker 600 MHz instrument using CDCl_3 (1, 2, and 6) and $\text{DMF-}d_7$ (4 and 5) as solvents. HR-ESIMS were run on a Thermoquest TLM LCQ Deca ion-trap spectrometer. Kromasil analytical, semipreparative, and preparative C_{18} columns (250 \times 4.5 mm, 250 \times 10 mm, and 250 \times 21.2 mm; i.d. 5 μm , Thermo) were used for preparative HPLC separations using a Waters autopurification system equipped with a binary pump (Waters 2525), a UV–vis diode array detector (190–600 nm, Waters 2996), and a PL-ELS 1000 ELSD Polymer Laboratory detector. Chiralpak analytical AD-H (150 \times 4.6 mm, 5 μm , Interchim) and semipreparative AD (250 \times 10 mm, 10 μm , Interchim) columns were used for diastereomer separations, using Waters Alliance 2695. SFC purification was performed on a Thar Waters SFC Investigator II System using a Waters 2998 photodiode array detector and a 2-ethylpyridine column (250 \times 4.6 mm, 5 μm , Princeton). Silica gel 60 (35–70 μm) and analytical TLC plates (Si gel 60 F 254) were purchased from SDS (France). A prepacked 140 g C_{18} Versapak cartridge was used for flash chromatography using a Combiflash-Companion apparatus (Serlabo). All other chemicals and solvents were purchased from SDS (France).

Computational Methods. Conformations (2000) of 2*R*,5'*R*- and 2*R*,5'*S*-configured Chartaceone A (1) were generated by the Monte Carlo²⁷ random search method and optimized by PRCG molecular mechanics minimization²⁸ using the MacroModel (version 5.5) program²⁹ with the OPLSA* force field³⁰ and GB/SA CHCl_3 solvation. Given the large degree of conformational freedom of the side chain, the conformational search led to a large number of structures, which could be classified in two main groups: folded side chain due to a hydrogen bond between the oxygen atom of the carboxylic acid and the 7-OH hydrogen or an extended side chain. Only the two most stable conformers of each group were selected for ab initio calculations. Gradient optimizations of these four structures using the B3LYP/6-31G(d,p) basis set^{31–34} have been performed with the Gaussian 03 program.³⁵ B3LYP calculations indicate that the two structures with hydrogen bonding are more stable (about 3 kcal/mol) than structures with the extended side chain. Consequently, for the sake of saving computational time, only structures with hydrogen bonding within a 3 kcal/mol range and the two most stable structures with the extended side chain were optimized at the B3LYP/6-31G(d,p) level. This selection was applied to both 2*R*,5'*R* and 2*R*,5'*S* configurations, leading, in each case, to a selection of six conformers. ECD calculations were performed, and, for both 2*R*,5'*R* and 2*R*,5'*S* configurations, ECD spectra predicted for the six conformations were added up with Boltzmann weighting³⁶ to give the calculated overall ECD spectrum. Boltzmann weighting and Gauss curve generation (using a sigma value of 0.16 eV) were done with SpecDis.³⁷

Plant Material. The trunk bark of *C. chartacea* was collected and identified by one of us (M.L.) in May 1998 at “Port Boisé”, South Province. The corresponding voucher specimen, LIT-0528, is kept at the Herbarium of the Botanical and Tropical Ecology Department of the IRD Center, Noumea, New Caledonia.

Extraction and Isolation. Air-dried powder of the bark (495 g) was extracted with EtOAc (3 \times 1.5 L) followed by MeOH (3 \times 1.5 L)

at room temperature. The EtOAc crude extract was concentrated in vacuo at 40 °C to yield 6 g of extract, which were subjected to C_{18} flash chromatography using a gradient of H_2O –MeOH–EtOAc (80:20:0 to 0:50:50) of decreasing polarity, leading to 12 fractions. Fraction 6 (144 mg; H_2O –MeOH, 30:70) was subjected to semipreparative HPLC on a C_{18} phase using H_2O –MeCN (50:50) at 15 $\text{mL}\cdot\text{min}^{-1}$ to afford pinocebrin (17.8 mg). Fraction 8 (2.3 g; H_2O –MeOH, 10:90) was subjected to silica gel CC using a gradient of CH_2Cl_2 –MeOH (100:0 to 80:20) of increasing polarity, leading to 17 fractions (F1'–F17') on the basis of TLC. Fraction 10' (359.3 mg; CH_2Cl_2 –MeOH, 99:1) was subjected to preparative HPLC on a C_{18} phase using H_2O –MeCN (24:76 + 0.1% HCO_2H) at 14 $\text{mL}\cdot\text{min}^{-1}$ to afford pinocebrin (4.7 mg), chartaceone A (1; 139.1 mg), and chartaceone B (2; 47.6 mg). Fraction 11' (370 mg; CH_2Cl_2 –MeOH, 98:2) was subjected to preparative HPLC on a C_{18} phase using H_2O –MeCN (20:80 + 0.1% HCO_2H) at 21 $\text{mL}\cdot\text{min}^{-1}$ to afford chartaceone A (1; 30.9 mg), chartaceone C (3; 48.1 mg), a mixture of chartaceones D and E (104.6 mg), and chartaceone F (6; 86.9 mg). A mixture of chartaceones D and E (38 mg) was subjected to semipreparative SFC on a 2-ethylpyridine phase using CO_2 –MeOH (70:30) at 10 $\text{mL}\cdot\text{min}^{-1}$, 39.9 °C, to afford chartaceone D (4; 8.2 mg) and chartaceone E (5; 9.7 mg). Chartaceone A (1; 85 mg) was subjected to semipreparative HPLC on a Chiralpak AD column using *n*-heptane–EtOH (70:30 + 0.1% HCO_2H) to afford chartaceones A1 (1a; 18.9 mg), A2 (1b; 21.7 mg), A3 (1c; 19.2 mg), and A4 (1d; 20.5 mg). Chartaceone B (2; 44.9 mg) was subjected to semipreparative HPLC on a Chiralpak AD column using *n*-heptane–EtOH (70:30 + 0.1% HCO_2H) to afford chartaceones B1 (10 mg), B2 (7.9 mg), B3 (11 mg), and B4 (7.8 mg).

Dengue 2 NS5 Polymerase Plasmid Constructs, Enzyme Preparation, and Reagents. Dengue 2 NS5 polymerase genes were tagged by six *N*-terminal histidine residues and expressed from the pQE30 vector (Quiagen) in *E. coli* Rosetta pLacI cells (Novagen). The enzymes were produced and purified as previously described.⁶ Homopolymeric cytosine Poly (rC) RNA template was obtained from GE-Healthcare (Mississauga, Canada). Uniformly labeled [³H]GTP (5.1 Ci/mmol) was purchased from Perkin (Boston, MA, USA).

Enzymatic Activity Assay of the Dengue Polymerase. Polymerase activity was assayed by monitoring the incorporation of radiolabeled guanosine into a homopolymeric cytosine RNA template, as previously described.⁶

Library Screening. The screening was conducted on plant extracts (barks, leaves) and their fractions. Quality of measurements was assessed by calculating the *Z'* factor for each plate: Z' factor = $1 - \frac{\{3\text{SD}(\text{neg}) + 3\text{SD}(\text{pos})\}}{[\text{av}(\text{neg}) - \text{av}(\text{pos})]}$, where SD(neg) and SD(pos) stand for the standard deviation obtained for negative and positive controls, respectively, and where av(neg) and av(pos) are averages for negative and positive controls, respectively. The *Z'* factor had an average value of 0.834 with a standard deviation of 0.058 for assay plates, indicating that there is a wide separation of data points between the baseline and positive signals. For each compound, the percentage of inhibition was calculated as follows: Inhibition % = $100(\text{raw_data_of_compound} - \text{av}(\text{pos})) / (\text{av}(\text{neg}) - \text{av}(\text{pos}))$. The library was organized in 96-wells plates, each containing 80 samples. Assay plates contained positive and negative controls distributed in the first and 12th columns, respectively. Our experimental screening consisted of an in vitro nucleotide incorporation assay in which a functionally active recombinant dengue NS5pol enzyme and a homopolymeric polycytosine template were used. Reactions were conducted in 20 μL volume. Positive and negative controls consisted of a reaction mixture (50 mM HEPES pH 8.0, 10 mM KCl, 2 mM MnCl_2 , 1 mM MgCl_2 , 10 mM DTT, 100 nM homopolymeric polycytosine RNA template, 20 nM NS5) supplemented by 10 μM [³H]-GTP (0.25 μCi) and 5% DMSO or 20 mM EDTA, respectively. For each assay, the enzyme mix was first distributed in plate wells using a BioMek 3000 workstation (Beckman). Each of 80 samples was added to the assay using a BioMek NX workstation (Beckman) to a final concentration of 50 $\mu\text{g}/\text{mL}$ in 5% DMSO. Reactions were initiated by addition of 10 μM [³H]-GTP (0.25 μCi), incubated at

30 °C, and stopped after 10 min by the addition of EDTA (100 mM final concentration). All distributions were conducted with the Biomek 3000. Reaction products were then transferred onto DE-81 paper membrane (Whatman International Ltd.) with a Packard Filtermate Harvester. Filter paper membranes were washed three times in 0.3 M ammonium formate (pH 8.0), washed twice with EtOH, and dried. The radioactivity bound to the filter was determined using liquid scintillation counting (Wallac Microbeta Trilux). Fractions or pure compounds showing 80% or more reaction inhibition were selected and used to generate new experimental plates. These experimental plates were used for a second screen at a 10 µg/mL final concentration, with the same experimental procedure. Compounds leading to an 80% inhibition or more in the second screen were qualified as hits. Hits were confirmed on purified freshly solubilized compound, and their IC₅₀'s determined.

IC₅₀ Determination. The compound concentration leading to 50% inhibition of NSS-mediated RNA synthesis was determined in the same buffer as the screen (cf. library screening section) containing 100 nM of homopolymeric cytosine RNA template, 40 nM of NSS, and various concentrations of compound (0; 0.1; 0.5; 1; 5; 10; 50 µM). Reactions incubated at 30 °C were initiated by the addition of 40 µM [³H]-GTP (0.2 µCi). After 5 min of incubation, the reaction was stopped by the addition of EDTA (100 mM final concentration). Reaction products were transferred onto a DE-81 paper membrane (Whatman International Ltd.) with a Packard Filtermate Harvester. Filter paper membranes were washed three times in 0.3 M ammonium formate (pH 8.0) and twice in EtOH and dried. Radioactivity bound to filters was determined using liquid scintillation counting (Wallac Microbeta Trilux). The residual activity for each condition was evaluated, and IC₅₀ was determined using the following equation: % of enzyme activity = 100/(1 + (I)²/IC₅₀), where I is the concentration of inhibitor. IC₅₀ was determined from curve-fitting using Kaleidagraph (Synergy Software). For each value, results were obtained using triplicates in a single experiment.

Cytotoxic Activity Determination. The cytotoxic activities of the compounds were evaluated against the KB (nasopharynx human carcinoma) cell line. Cytotoxicity assays were performed according to a published procedure.³⁸ Taxotere was used as a reference compound (IC₅₀ of 15 nM on KB).

(±)-Chartaceone A (1): yellow, amorphous solid; UV (MeOH) λ_{max} (log ε) 341 (sh) (3.6), 294 (4.26), 255 (4.36) nm; ¹H and ¹³C NMR, see Tables 1 and 2; HR-ESIMS *m/z* 457.1671 [M – H][–] (calcd for C₂₈H₂₅O₆, 457.1651).

Chartaceone A1 (1a): [α]_D²⁵ +82 (c 1, CHCl₃); CD (MeOH, c 1.15 × 10^{–3}) λ_{max} (Δε) 331 (–1.72), 287 (19.39), 256 (18.00), 220 (–35.05) nm; ¹H and ¹³C NMR, see Tables 1 and 2.

Chartaceone A2 (1b): [α]_D²⁵ –56 (c 0.5, CHCl₃); CD (MeOH, c 1.15 × 10^{–3}) λ_{max} (Δε) 331 (–4.62), 289 (7.60), 255 (–25.51), 233 (24.68) nm; ¹H and ¹³C NMR, see Tables 1 and 2.

Chartaceone A3 (1c): [α]_D²⁵ +56 (c 0.5, CHCl₃); CD (MeOH, c 1.15 × 10^{–3}) λ_{max} (Δε) 328 (3.41), 290 (–3.94), 255 (24.68), 233 (–14.16) nm; ¹H and ¹³C NMR, see Tables 1 and 2.

Chartaceone A4 (1d): [α]_D²⁵ –88 (c 1, CHCl₃); CD (MeOH, c 1.15 × 10^{–3}) λ_{max} (Δε) 330 (2.76), 287 (–11.70), 257 (–9.25), 220 (30.02) nm; ¹H and ¹³C NMR, see Tables 1 and 2.

(±)-Chartaceone B (2): yellow, amorphous solid; UV (MeOH) λ_{max} (log ε) 341 (sh) (3.54), 294 (4.21) nm; ¹H and ¹³C NMR, see Tables 1 and 2; HR-ESIMS *m/z* 457.1653 [M – H][–] (calcd for C₂₈H₂₅O₆, 457.1651).

Chartaceone B1: [α]_D²⁵ –31 (c 0.5, CHCl₃); CD (MeOH, c 1.25 × 10^{–3}) λ_{max} (Δε) 331 (–1.42), 290 (6.16), 220 (–10.80) nm.

Chartaceone B2: [α]_D²⁵ +45 (c 0.5, CHCl₃); CD (MeOH, c 1.25 × 10^{–3}) λ_{max} (Δε) 330 (–0.74), 289 (3.10), 221 (–2.77) nm.

Chartaceone B3: [α]_D²⁵ –48 (c 0.5, CHCl₃); CD (MeOH, c 1.25 × 10^{–3}) λ_{max} (Δε) 329 (0.98), 290 (–5.06), 220 (5.02) nm.

Chartaceone B4: [α]_D²⁵ +35 (c 0.5, CHCl₃); CD (MeOH, c 1.25 × 10^{–3}) λ_{max} (Δε) 329 (0.89), 288 (–4.80), 218 (8.60) nm.

(±)-Chartaceone C (3): yellow-orange, amorphous solid; UV (MeOH) λ_{max} (log ε) 341.5 (sh) (3.60), 295.5 (3.97) nm; ¹H and ¹³C

NMR, see Tables 1 and 2; HR-ESIMS *m/z* 659.2653 [M – H][–] (calcd for C₄₁H₃₉O₈, 659.2645).

(±)-Chartaceone D (4): brownish, amorphous solid; UV (MeOH) λ_{max} (log ε) 340.5 (sh) (3.52), 294 (4.07), 254 (4.23) nm; ¹H and ¹³C NMR, see Tables 1 and 2; HR-ESIMS *m/z* 659.2689 [M – H][–] (calcd for C₄₁H₃₉O₈, 659.2645).

(±)-Chartaceone E (5): brownish, amorphous solid; UV (MeOH) λ_{max} (log ε) 341.5 (sh) (3.51), 294.5 (4.01), 254 (4.18) nm; ¹H and ¹³C NMR, see Tables 1 and 2; HR-ESIMS *m/z* 659.2653 [M – H][–] (calcd for C₄₁H₃₉O₈, 659.2645).

(±)-Chartaceone F (6): yellow-orange, amorphous solid; UV (MeOH) λ_{max} (log ε) 340.5 (sh) (3.76), 294 (4.24), 250 (4.48) nm; ¹H and ¹³C NMR, see Tables 1 and 2; HR-ESIMS *m/z* 659.2603 [M – H][–] (calcd for C₄₁H₃₉O₈, 659.2645).

■ ASSOCIATED CONTENT

📄 Supporting Information

NMR spectra for compounds 1–6, chromatograms for compounds 1 and 2, and experimental ECD spectra for chartaceones B1–B4 are available free of charge via the Internet at <http://pubs.acs.org>.

■ ACKNOWLEDGMENTS

The authors are grateful to South Province of New Caledonia, which facilitated our field investigation. We express our thanks to G. Aubert (ICSN), who performed the cytotoxicity assays on the KB cell line and M.-T. Martin (ICSN) for her help and advice in NMR studies. AFMB thanks the Région PACA, the Association de Recherche contre le Cancer (ARC), the Infectiopole, the Université de la Méditerranée (BQR), the Direction Générale de l'Armement (DGA), the Agence Nationale de la Recherche (ANR), and the Fondation pour la Recherche Médicale (FRM, Aide aux Équipes) for their support. They also thank B. Selisko for her contribution as operating manager of the PCML platform and M. Blemont for the screening.

■ REFERENCES

- Guzmán, M. G.; Kourí, G. *Lancet Infect. Dis.* **2002**, *2*, 33–42.
- Guzmán, M. G.; Halstead, S. B.; Artsob, H.; Buchy, P.; Farrar, J.; Gubler, D. J.; Hunsperger, E.; Kroeger, A.; Margolis, H. S.; Martínez, E.; Nathan, M. B.; Pelegrino, J. L.; Simmons, C.; Yoksan, S.; Peeling, R. W. *Nat. Rev. Microbiol.* **2010**, *8*, 7–16.
- Coller, B.-A. G.; Clements, D. E. *Curr. Opin. Immunol.* **2011**, *23*, 391–398.
- Malet, H.; Massé, N.; Selisko, B.; Romette, J.-L.; Alvarez, K.; Guillemot, J. C.; Tolou, H.; Yap, T. L.; Vasudevan, S.; Lescar, J.; Canard, B. *Antivir. Res.* **2008**, *80*, 23–35.
- Niyomrattanakit, P.; Chen, Y.-L.; Dong, H.; Yin, Z.; Qing, M.; Glickman, J. F.; Lin, K.; Mueller, D.; Voshol, H.; Lim, J. Y. H.; Nilar, S.; Keller, T. H.; Shi, P.-Y. *J. Virol.* **2010**, *84*, 5678–5686.
- Selisko, B.; Dutartre, H.; Guillemot, J.-C.; Debarnot, C.; Benarroch, D.; Khromykh, A.; Desprès, P.; Eglouff, M.-P.; Canard, B. *Virology* **2006**, *351*, 145–158.
- Awang, K.; Hadi, A. H. A.; Saidi, N.; Mukhtar, M. R.; Morita, H.; Litaudon, M. *Fitoterapia* **2008**, *79*, 308–310.
- Toribio, A.; Bonfils, A.; Delannay, E.; Prost, E.; Harakat, D.; Henon, E.; Richard, B.; Litaudon, M.; Nuzillard, J. M.; Renault, J. H. *Org. Lett.* **2006**, *8*, 3825–3828.
- Cavalheiro, A. J.; Yoshida, M. *Phytochemistry* **2000**, *53*, 811–819.
- Drewes, S. E.; Sehlapelo, B. M.; Horn, M. M.; Scott-shaw, R.; Sandor, P. *Phytochemistry* **1995**, *38*, 1427–1430.
- Chou, T.-H.; Chen, J.-J.; Lee, S.-J.; Chiang, M. Y.; Yang, C.-W.; Chen, I.-S. *J. Nat. Prod.* **2010**, *5*, 6–11.
- Fu, X.; Sévenet, T.; Remy, F.; Païs, M.; Hadi, A. H. A.; Zeng, L. *J. Nat. Prod.* **1993**, *56*, 1153–1163.

- (13) Dumontet, V.; Gaspard, C.; Van Hung, N.; Fahy, J.; Tchertanov, L.; Sévenet, T.; Guéritte, F. *Tetrahedron* **2001**, *57*, 6189–6196.
- (14) Dumontet, V.; Van Hung, N.; Adeline, M. T.; Riche, C.; Chiaroni, A.; Sévenet, T.; Guéritte, F. *J. Nat. Prod.* **2004**, *67*, 858–862.
- (15) Wang, K.; Hu, Y.; Liu, Y.; Mi, N.; Fan, Z.; Liu, Y.; Wang, Q. *J. Agric. Food Chem.* **2010**, *58*, 12337–12342.
- (16) Yang, C.-W.; Lee, Y.-Z.; Kang, I.-J.; Barnard, D. L.; Jan, J.-T.; Lin, D.; Huang, C.-W.; Yeh, T.-K.; Chao, Y.-S.; Lee, S.-J. *Antivir. Res.* **2010**, *88*, 160–168.
- (17) Min, H.-Y.; Chung, H.-J.; Kim, E.-H.; Kim, S.; Park, E.-J.; Kook, S. *Biochem. Pharmacol.* **2010**, *80*, 1356–1364.
- (18) Chen, Y.-C.; Kung, F.-L.; Tsai, I.-L.; Chou, T.-H.; Chen, I.-S.; Guh, J.-H. *J. Urol.* **2010**, *183*, 2409–2418.
- (19) Andersen, Ø. M.; Markham, K. R. *Flavonoids: Chemistry, Biochemistry, and Applications*; CRC Press, 2006; p 917.
- (20) Lewis, F. D.; Zuo, X. *J. Am. Chem. Soc.* **2003**, *125*, 8806–8813.
- (21) Slade, D.; Ferreira, D.; Marais, J. P. J. *Phytochemistry* **2005**, *66*, 2177–2215.
- (22) Gaffield, W. *Tetrahedron* **1970**, *26*, 4093–4108.
- (23) Su, B.-N.; Park, E. J.; Vigo, J. S.; Graham, J. G.; Cabieses, F.; Fong, H. H. S.; Pezzuto, J. M.; Kinghorn, A. D. *Phytochemistry* **2003**, *63*, 335–341.
- (24) Ding, Y.; Li, X.-C.; Ferreira, D. *J. Org. Chem.* **2007**, *72*, 9010–9017.
- (25) Ding, Y.; Li, X.-C.; Ferreira, D. *J. Nat. Prod.* **2009**, *72*, 327–335.
- (26) Prasain, J.; Li, J.; Tezuka, Y.; Tanaka, K.; Basnet, P.; Dong, H.; Namba, T.; Kadota, S. *J. Nat. Prod.* **1998**, *61*, 212–216.
- (27) Chang, G.; Guida, W. C.; Still, W. C. *J. Am. Chem. Soc.* **1989**, *111*, 4379–4386.
- (28) Polak, E.; Ribiere, G. *Rev. Fr. Inform. Rech. O.* **1969**, *3*, 35–43.
- (29) Mohamadi, F.; Richards, N. G. J.; Guida, W. C.; Liskamp, R.; Lipton, M.; Caufield, C.; Chang, G.; Hendrickson, T.; Still, W. C. *J. Comput. Chem.* **1990**, *11*, 440–467.
- (30) Jorgensen, W. L.; Tirado-Rives, J. *J. Am. Chem. Soc.* **1988**, *110*, 1657–1666.
- (31) Becke, A. D. *J. Chem. Phys.* **1993**, *98*, 5648.
- (32) Hariharan, P. C.; Pople, J. A. *Theor. Chim. Acta* **1973**, *28*, 213–222.
- (33) Petersson, G.; Bennett, A.; Tensfeldt, T. G.; Al-Laham, M.; Shirley, W.; Mantzaris, J. *J. Chem. Phys.* **1988**, *89*, 2193–2218.
- (34) Petersson, G. A.; Al-Laham, M. A. *J. Chem. Phys.* **1991**, *94*, 6081–6091.
- (35) Frisch, M. J.; Trucks, G. W.; Schlegel, H. B.; Scuseria, G. E.; Robb, M. A.; Cheeseman, J. R.; Montgomery, J. A., Jr.; Vreven, T.; Kudin, K. N.; Burant, J. C.; Millam, J. M.; Iyengar, S. S.; Tomasi, J.; Barone, V.; Mennucci, B.; Cossi, M.; Scalmani, G.; Rega, N.; Petersson, G. A.; Nakatsuji, H.; Hada, M.; Ehara, M.; Toyota, K.; Fukuda, R.; Hasegawa, J.; Ishida, M.; Nakajima, T.; Honda, Y.; Kitao, O.; Nakai, H.; Klene, M.; Li, X.; Knox, J. E.; Hratchian, H. P.; Cross, J. B.; Bakken, V.; Adamo, C.; Jaramillo, J.; Gomperts, R.; Stratmann, R. E.; Yazyev, O.; Austin, A. J.; Cammi, R.; Pomelli, C.; Ochterski, J. W.; Ayala, P. Y.; Morokuma, K.; Voth, G. A.; Salvador, P.; Dannenberg, J. J.; Zakrzewski, V. G.; Dapprich, S.; Daniels, A. D.; Strain, M. C.; Farkas, O.; Malick, D. K.; Rabuck, A. D.; Raghavachari, K.; Foresman, J. B.; Ortiz, J. V.; Cui, Q.; Baboul, A. G.; Clifford, S.; Cioslowski, J.; Stefanov, B. B.; Liu, G.; Liashenko, A.; Piskorz, P.; Komaromi, I.; Martin, R. L.; Fox, D. J.; Keith, T.; Al Laham, M. A.; Peng, C. Y.; Nanayakkara, A.; Challacombe, M.; Gill, P. M. W.; Johnson, B.; Chen, W.; Wong, M. W.; Gonzalez, C.; Pople, J. A. *Gaussian03, revision C.02*; Gaussian, Inc.: Wallingford, CT, 2004.
- (36) Bringmann, G.; Bruhn, T.; Maksimenka, K.; Hemberger, Y. *Eur. J. Org. Chem.* **2009**, 2717–2727.
- (37) Bruhn, T.; Hemberger, Y.; Schaumlöffel, A.; Bringmann, G. *SpecDis*, Version 1.51; University Würzburg: Würzburg, Germany, 2011.
- (38) Tempête, C.; Werner, G.; Favre, F.; Rojas, A.; Langlois, N. *Eur. J. Med. Chem.* **1995**, *30*, 647–650.